ChemComm

Accepted Manuscript

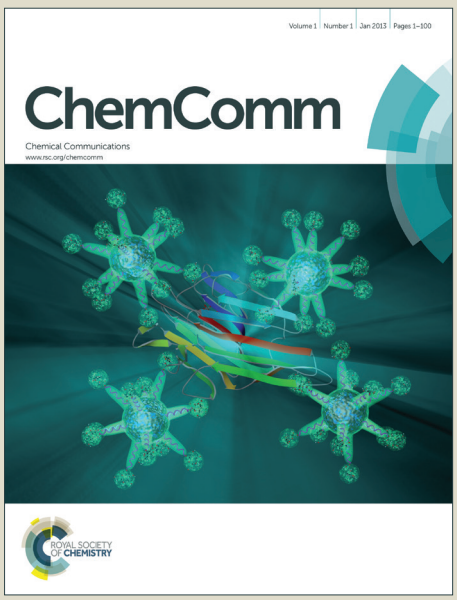

ROYAL SOCIETY OF CHEMISTRY

www.rsc.org/chemcomm

Journal Name

RSCPublishing

COMMUNICATION

DNA-regulated silver nanoclusters for label-free ratiometric fluorescence detection of DNA†

Cite this: DOI: 10.1039/x0xx00000x

Lin Liu, Qianhui Yang, Jianping Lei,* Nan Xu and Huangxian Ju

Received 00th January 2014,
Accepted 00th January 2014

DOI: 10.1039/x0xx00000x

www.rsc.org/

Two kinds of DNA-regulated Ag nanoclusters were one-pot synthesized on an oligonucleotide, and delicately utilized in the design of label-free ratiometric fluorescence strategy for DNA detection with simplicity and high sensitivity.

Ratiometric fluorescence technique has attracted much attention in the detection of complex samples through recording the ratio of fluorescence intensities at two different wavelengths.[1] Compared to steady-state fluorescence (FL), ratiometric fluorescence detection can minimize the environmental inferring factors, and thus the more accurate and effective detection can be achieved.[2-6] There are two kinds of mechanisms generally utilized in ratiometric fluorescence detection. One is on the basis of emission change in response to the targets using organic dyes as fluorophores.[7-12] Typically, Lippard et al. have reported a red-emitting organic probe for turn-on and ratiometric fluorescence detection of Hg^{2+} in aqueous solution.[2] Kim et al. used a benzimidazole derivative as ratiometric two-photon fluorescent probe to monitor acidic pH values by the blue-to-green emission color change.[9] The other mechanism is based on fluorescence resonance energy transfer (FRET) between the dye and nanomaterials.[13] Utilizing two kinds of fluorophores with energy donor–acceptor architectures can achieve larger pseudo-Stokes shifts than that of single fluorophores. For example, a specific ratiometric fluorescence has designed for detection of protein through FRET between CdSe–ZnS core–shell quantum dot and dye acceptor.[14] Although the above ratiometric fluorescence methods have achieved the good performance for the detection of targets, the need of labeled fluorescent probe, the poor anti-bleaching, or construction of donor–acceptor pairs limited their applications in practice.

With the development of nanoscience and nanotechnology, fluorescence nanomaterials demonstrate some distinguished advantages in the design of ratiometric fluorescence probe. A binary heterogeneous nanocomplex of gold clusters and carbon dots was constructed for ratiometric detection of highly reactive oxygen species.[15] On the other hand, silver nanoclusters (Ag NCs) are a promising option as fluorophores due to the regulative property of Ag NCs, especially for using DNA as template. Since there is a high affinity between Ag^+ and cytosine base (C base), Ag NCs could be generated straightly from C-rich oligonucleotides through simply reduction of Ag^+, which allows the demission of labeling.[16] What's more, fluorescent properties of DNA-templated Ag NCs are largely sequence-,[17,18] and structure-dependent.[19-22] The formation of fluorescent Ag NCs in hybridized DNA duplex scaffolds can identify a typical single-nucleotide mutation.[23] Herein, using DNA as template, two kinds of Ag NCs were one-pot synthesized on an oligonucleotide, and delicately utilized in the design of label-free ratiometric fluorescent strategy for DNA detection.

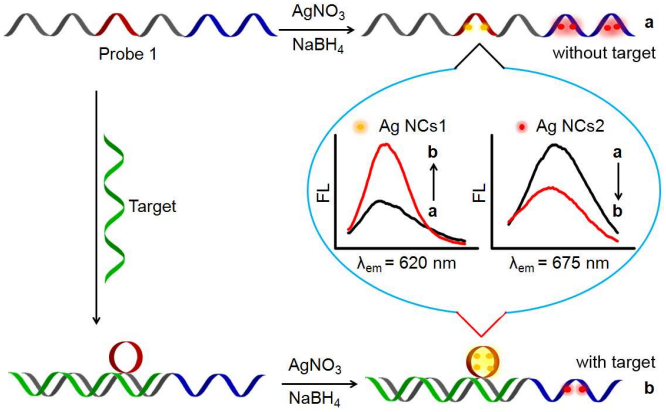

Scheme 1 Schematic illustration of label-free ratiometric fluorescence strategy utilizing DNA-regulated Ag NCs for DNA detection.

First, the sequence of probe 1 was delicately tailored to contain two regions (Scheme 1), which could simultaneously generate two kinds of silver nanoclusters (Ag NCs1 and Ag NCs2) with different fluorescence properties in presence of $NaBH_4$. When target DNA was introduced, the red region of probe 1 could turn into a loop which enhanced fluorescence intensity of Ag NCs1[23] while the fluorescent intensity of Ag NCs2 originated from the blue region decreased. The ratios of two fluorescence intensities at different emission wavelengths could be used to quantify the concentration of target DNA in a sensitive way.

The feasibility of the proposed method was identified by the spectral change in response to targets. The probe 1 (1 μM) alone demonstrated two emission peaks at 620 nm and 675 nm with excitation wavelengths of 550 nm and 600 nm for Ag NCs1 and Ag NCs2, respectively (Fig. S1). With the increasing of target DNA

concentrations, the fluorescence intensity of Ag NCs1 (F_{620}) was greatly enhanced (Fig. 1A, curves b and c) while the fluorescence intensity of Ag NCs2 (F_{675}) was obviously reduced (Fig. 1B, curves b and c). The opposite change of fluorescence intensities led to the large ratios of F_{620}/F_{675} for ratiometric fluorescence detection of target DNA with convenience and sensitivity.

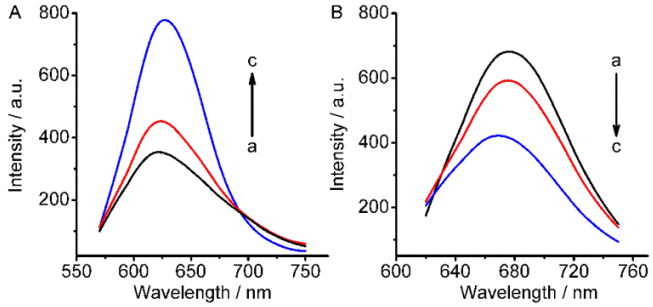

Fig. 1 Fluorescent spectra of (A) Ag NCs1 and (B) Ag NCs2 generated from 1 μM probe 1 (a), 1 μM probe 1 + 250 nM target DNA (b), and 1 μM probe 1 + 1 μM target DNA (c).

To identify the functions of the sequences in red and blue regions, three kinds of probes were designed for generation of the fluorescent Ag NCs (Table 1). First, for probe X, which was just the complement oligonucleotide of target DNA, none fluorescence emissions were observed in the presence/absence of target DNA (Fig. 2A and D). This result suggested that the sequence of probe X couldn't be templated the generation of fluorescent Ag NCs even in the presence of abundant C bases. Second, probe R containing the red part more than probe X, could only generate Ag NCs1 alone as predicted (Fig. 2B and E, black). Introducing target DNA to probe R caused a dramatically increase in fluorescence intensity of Ag NCs1 (Fig. 2B, red), because the red part turned into a loop to enhance fluorescence emission.[23] As for the probe (probe B) containing the blue part more than probe X, the strong fluorescence emission of Ag NCs2 was observed along with weak fluorescence emission of Ag NCs1 (Fig. 2C and F, black). However, after hybridizing with target, the fluorescence intensities of both Ag NCs1 and Ag NCs2 reduced obviously due to the formation of the duplex, which was consistent with the previous report.[24] Therefore, it could be conducted that the conformation of red and blue regions regulated the generation of Ag NCs, providing a possibility in design of label-free ratiometric fluorescence method for detection of DNA.

Table 1. Oligonucleotides employed in this work.

Oligonucleotides	Oligonucleotides Sequence (5´- 3´)
Probe 1	TATTAACTTTACTCCCTTACCCTTCCTCCCCG CTGATTTTCCCCTTTT
Target	TCAGCGGGGAGGAAGGGAGTAAAGTTAATA
Probe B	TATTAACTTTACTCCCTTCCTCCCCGCTGATT TTCCCCTTTT
Probe R	TATTAACTTTACTCCCTTACCCTTCCTCCCCG CTGA
Probe X	TATTAACTTTACTCCCTTCCTCCCCGCTGA

The red and blue parts of Probe represent the loop and 3´-end sequences for generating two different kinds of Ag NCs, respectively.

To analyze the internal relationship between the sequence of the loop and Ag NC1, the probes with different loop sequences were studied (Table S1). Probe RA, which was designed through deleting A base from the loop of probe R, could not generate any fluorescent Ag NCs in the presence/absence of target DNA (Fig. S2, black), inferring that A base in the loop was important for the generation of the fluorescent Ag NCs. Subsequently, by replacing A base with G, T and C bases, probe RG, probe RT and probe RC were designed, respectively. Probe RG and RT could not make obvious difference from probe RA (Fig. S2, green and blue) while probe RC generated strong fluorescence emission of Ag NCs1 (Fig. S2, red). However, for probe RC, the introducing of target could not lead to an obvious fluorescence enhancement. Therefore, the A base in the loop was no substitute in design of the probe for ratiometric fluorescence detection.

In order to obtain good performance, the concentration of probe 1, vibrating time of $NaBH_4$ and pH during Ag NCs synthesis were optimized. As shown in Fig. S3A, the fluorescence intensity increased linearly along with the concentrations of probe 1. Considering the accuracy and economy of detection, 1 μM was chosen as the optimal concentration of probe 1 in detection procedure. The vibrating time of $NaBH_4$ was also optimized in the range of 3 to 30 min. Obviously, the vibrating for 15 min resulted in largely difference of fluorescent ratios for two Ag NCs (Fig. S3B). The pH during Ag NCs synthesis was an important factor to affect the fluorescence intensity of DNA-regulated Ag NCs. The fluorescent ratio of Ag NCs1 increased with the increasing of pH from 6.5 to 8.0, while the fluorescent ratio of Ag NCs2 decreased with the increasing of pH up to 7.5 (Fig. S3C). Therefore, 20 mM pH 7.5 Tri-HCl buffer was used throughout the following experiments.

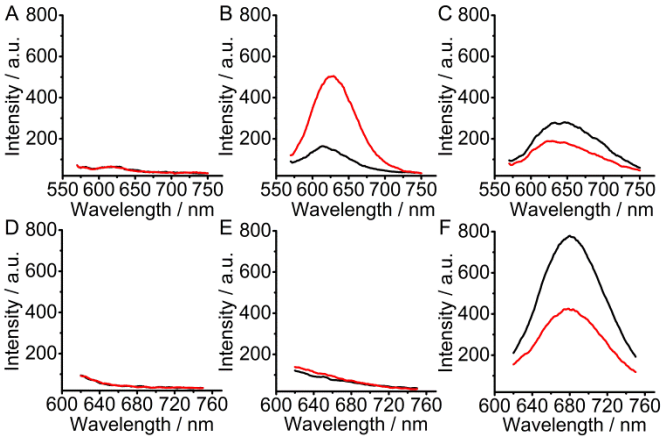

Fig. 2 Fluorescent spectra of (A, B, C) Ag NCs1 and (D, E, F) Ag NCs2 generated by utilizing 1 μM probe X (A, D), probe R (B, E) and probe B (C, F) with (red line) and without (black line) 1 μM target DNA.

The synthesized Ag NCs were characterized with transmission electron microscopy. The size of Ag NCs1 generated from probe B is slightly smaller than that of probe R (~ 2 nm) with homogenous distribution (Fig. S4B and C). In addition, the more density Ag NCs originated from probe 1 were observed (Fig. S4A). These results identified the formation of two different Ag NCs in DNA template.

At the optimized conditions, target DNA of different concentrations from 0 to 1000 nM was detected. The ratio of fluorescence intensities was proportional to target concentration ranging from 10 to 1000 nM (Fig. 3). The linear regression equation was $I = 0.515 + 0.00134 \times c$ ($R^2 = 0.991$), where I was the ratio of fluorescence intensities of Ag NCs1 and Ag NCs2, and c was the concentration of target DNA. The limit of detection was estimated at 3σ calculated in the absence of target to be 7.3 nM, which was lower than steady-state fluorescence DNA sensing strategies using DNA-templated Ag NCs[25,26] or ratiometric fluorescence method.[7]

The specificity of this ratiometric fluorescence strategy combining Ag NCs was demonstrated to be acceptable for discriminating the three-base mismatched DNA from the complementary target (Fig. S5). Also, the positions of the mismatched bases could be figured out

through comparing the change of fluorescence intensity for Ag NC1 and Ag NCs2. When the mismatched bases were near the loop (Table S1, R-tm target), which might influence the formation of the loop, the enhancement of fluorescence intensity of Ag NCs1 caused by R-tm target was only as much as 25% of the same concentration complementary target. Meanwhile, the R-tm target had no effect on the formation of Ag NCs2. Similarly, when the mismatched bases were near the blue region (Table S1, B-tm target), the decrease of fluorescence intensity of Ag NCs2 was as much as 60% of the same concentration complementary target, and the enhancement of fluorescence intensity of Ag NCs1 was the same with the complementary target's. The ratiometric strategy can enlarge the difference between mismatch DNA and target DNA. Thus the dual fluorescence change provides a reliable method for discriminating the mismatched DNA in DNA detection.

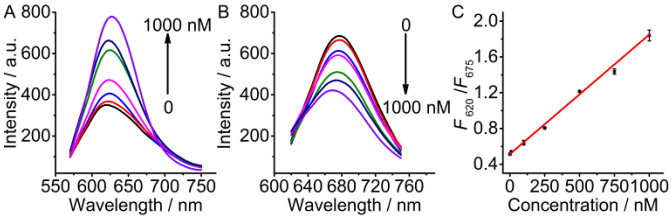

Fig. 3 Fluorescence spectra of (A) Ag NCs1 and (B) Ag NCs2 using 1 μM probe 1 as template at 0, 10, 100, 250, 500, 750, 1000 nM target. (C) Calibration curve of fluorescence intensity ratio of F_{620} to F_{675} *vs* target DNA concentration.

To test the validity of the proposed assay in the clinical sample, recovery testing was carried out by spiking target DNA solution into human serum. At the concentration of 500 nM, the recovery is 92.0 ± 2.9% (n = 3), indicating that the proposed ratiometric strategy for DNA detection could be used in real sample analysis.

This work developed the label-free ratiometric fluorescence strategy based on DNA-regulated Ag nanoclusters for sensitive detection of DNA. By regulating the conformation of the probe, two kinds of Ag NCs were successfully one-pot prepared with different fluorescence properties. When introducing target DNA, the red region turned into a loop so that the fluorescence intensity of Ag NCs1 was enhanced. Meanwhile, fluorescence intensity of Ag NCs2 decreased due to the formation of duplex. The opposite change led to the large ratios of two fluorescence intensities from Ag NCs, and thus was used to sensitively quantify target DNA in a ratiometric way. Interestingly, the mismatched bases could be effectively positioned through comparing the fluorescence change of Ag NCs1 and Ag NCs2. In addition, the different sequence of the loop resulted in the different fluorescence response to the targets, and thus this phenomenon could be potential for the distinguishing of single nucleotide polymorphism. The nanomaterials-based ratiometric fluorescence method can overcome the disadvantages of the organic fluorescent probe, and expand the application of fluorescent detection in bioimaging and bioanalysis.

This research was financially supported by the National Basic Research Program of China (2010CB732400), and the National Natural Science Foundation of China (21375060, 21135002, 21121091).

Notes and references

State Key Laboratory of Analytical Chemistry for Life Science, School of Chemistry and Chemical Engineering, Nanjing University, Nanjing 210093, P.R. China.
E-mail: jpl@nju.edu.cn; Fax: +86 25 83593593; Tel: +86 25 83593593
† Electronic Supplementary Information (ESI) available: Experimental details and additional figures. See DOI: 10.1039/c000000x/

1. (a) J. L. Fan, M. M. Hu, P. Zhan and X. J. Peng, *Chem. Soc. Rev.*, 2013, **42**, 29–43; (b) K. M. Wang, X. X. He, X. H. Yang and H. Shi, *Accounts Chem. Res.*, 2013, **46**, 1367–1376; (c) K. Kikuchi, *Chem. Soc. Rev.*, 2010, **39**, 2048–2053; (d) C. J. Chang, J. Jaworski, E. M. Nolan, M. Sheng and S. J. Lippard, *Proc. Natl. Acad. Sci.*, 2004, **101**, 1129–1134; (e) G. Q. Zhang, G. M. Palmer, M. W. Dewhirst and C. L. Fraser, *Nat. Mater.*, 2009, **8**, 747–751.
2. E. M. Nolan and S. J. Lippard, *J. Am. Chem. Soc.*, 2007, **129**, 5910–5918.
3. X. F. Hou, Q. X. Yu, F. Zeng, C. M. Yu and S. Z. Wu, *Chem. Commun.*, 2014, **50**, 3417–3420.
4. C. M. Yu, X. Z. Li, F. Zeng, F. Y. Zheng and S. Z. Wu, *Chem. Commun.*, 2013, **49**, 403–405.
5. C. Q. Ding, A. W. Zhu and Y. Tian, *Accounts Chem. Res.*, 2013, **47**, 20–30.
6. A. W. Zhu, Q. Qu, X. L. Shao, B. Kong and Y. Tian, *Angew. Chem. Int. Ed.*, 2012, **124**, 7297–7301.
7. L. M. Huang and S. W. Tam-Chang, *Chem. Commun.*, 2011, **47**, 2291–2293.
8. T. Yoshihara, Y. Yamaguchi, M. Hosaka, T. Takeuchi and S. Tobita, *Angew. Chem. Int. Ed.*, 2012, **51**, 4148–4151.
9. H. J. Kim, C. H. Heo and H. M. Kim, *J. Am. Chem. Soc.*, 2013, **135**, 17969–17977.
10. E. G. Matveeva, Z. Gryczynski, D. R. Stewart and I. Gryczynski, *J. Lumin.*, 2009, **129**, 1281–1285.
11. J. Ueberfeld and D. R. Walt, *Anal. Chem.*, 2004, **76**, 947–952.
12. P. J. Santangelo, B. Nix, A. Tsourkas and G. Bao, *Nucleic Acids Res.*, 2004, **32**, e57.
13. (a) X. J. Liu, N. Zhang, T. Bing and D. H. Shangguan, *Anal. Chem.,* 2014, **86**, 2289–2296; (b) C. M. Tyrakowski and P. T. Snee, *Anal. Chem.,* 2014, **86**, 2380–2386; (c) J. F. Han, C. Zhang, F. Liu, B. H. Liu, M. Y. Han, W. S. Zou, L. Yang and Z. P. Zhang, *Analyst*, 2014, **139**, 3032–3038; (d) Y. Zhou, W. B. Pei, C. Y. Wang, J. X. Zhu, J. S. Wu, Q. Y. Yan, L. Huang, W. Huang, C. Yao, J. S. C. Loo and Q. C. Zhang, *Small*, 2014, doi:10.1002/smll.201303127.
14. H. Y. Zhang, G. Q. Feng, Y. Guo and D. J. Zhou, *Nanoscale*, 2013, **5**, 10307–10315.
15. E. G. Ju, Z. Liu, Y. D. Du, Y. Tao, J. S. Ren and X. G. Qu, *ACS Nano*, 2014, doi:10.1021/nn501135m.
16. J. T. Petty, J. Zheng, N. V. Hud and R. M. Dickson, *J. Am. Chem. Soc.*, 2004, **126**, 5207–5212.
17. B. Sengupta, C. M. Ritchie, J. G. Buckman, K. R. Johnsen, P. M. Goodwin and J. T. Petty, *J. Phys. Chem. C*, 2008, **112**, 18776–18782.
18. J. Sharma, R. C. Rocha, M. L. Phipps, H. Yeh, K. A. Balatsky, D. M. Vu, A. P. Shreve, J. H. Werner and J. S. Martinez, *Nanoscale*, 2012, **4**, 4107–4110.
19. Z. X. Zhou, Y. Q. Liu and S. J. Dong, *Chem. Commun.*, 2013, **49**, 3107–3109.
20. L. Y. Feng, Z. Z. Huang, J. S. Ren and X. G. Qu, *Nucleic Acids Res.*, 2012, **40**, e122.
21. B. Sengupta, K. Springer, J. G. Buckman, S. P. Story, O. H. Abe, Z. W. Hasan, Z. D. Prudowsky, S. E. Rudisill, N. N. Degtyareva and J. T. Petty, *J. Phys. Chem. C*, 2009, **113**, 19518–19524.
22. T. Li, L. B. Zhang, J. Ai, S. J. Dong and E. K. Wang, *ACS Nano*, 2011, **5**, 6334–6338.
23. W. W. Guo, J. P. Yuan, Q. Z. Dong and E. K. Wang, *J. Am. Chem. Soc.*, 2010, **132**, 932–934.
24. (a) S. W. Yang and T. Vosch, *Anal. Chem.*, 2011, **83**, 6935–6939; (b) P. Shah, P. W. Thulstrup, S. K. Cho, Y. J. Bhang, J. C. Ahn, S. W. Choi, M. J. Bjerrum and S. W. Yang, *Analyst*, 2014, **139**, 2158–2166; (c) P. Shah, A. Rørvig-Lund, S. B. Chaabane, P. W. Thulstrup, H. G. Kjaergaard, E. Fron, J. Hofkens, S. W. Yang and T. Vosch, *ACS Nano*, 2012, **6**, 8803–8814.
25. L. B. Zhang, J. B. Zhu, Z. X. Zhou, S. J. Guo, J. Li, S. J. Dong and E. K. Wang, *Chem. Sci.*, 2013, **4**, 4004–4010.
26. G. Y. Lan, W. Y. Chen and H. T. Chang, *Biosens. Bioelectron.*, 2011, **26**, 2431–2435.